# Improvement of the Bondability of Wheat Straw Treated by Water Vapor Plasma for Bio-composites Manufacture

Yicheng Xu, Minzhi Chen, and Xiaoyan Zhou *

Wheat straw (WS) was first modified with water vapor plasma to enhance its interfacial bonding performance. The treatment effects during the entire exposing process were investigated in terms of surface wettability, physicochemical characteristics, and mechanical properties of glued test-pieces (three different forms) using contact angle analysis, free energy analysis, scanning electron microscopy (SEM), atomic force microscopy (AFM), X-ray photoelectron spectroscopy (XPS), and shear strength analysis. The results showed that 180 s of plasma treatment time resulted in a low instantaneous and equilibrium contact angle of urea-formaldehyde (UF) – 40.8% and 46.5% lower, respectively, in comparison with that of the untreated WS exterior surface. Obvious etching morphology was observed on the WS surfaces and positive activation was detected, demonstrating a remarkable increase in the surface free energy and O/C ratio. With the water vapor plasma treatment, the use of electrochemical reaction to introduce polar groups and etching to produce glue nails, were effective methods for improving the bonding performance of the WS.

*Keywords: Wheat straw; Water vapor plasma; Wettability; Bonding performance; Morphology; Surface chemistry*

*Contact information: College of Materials Science and Engineering, Nanjing Forestry University, Nanjing 210037, China; *Corresponding author: zhouxiaoyan@njfu.edu.cn*

## INTRODUCTION

Massive deforestation on a global scale has caused serious natural resource depletion and environmental pressures, which hinder the sustainable development of human life (Damette and Delacote 2011; Yildirim *et al.* 2014). These negative impacts, which are partially attributable to the wood-based panel industry, have prompted great interest in renewable, inexpensive, and substitute raw materials (Xu *et al.* 2004). There is a huge annual worldwide production of agricultural residues such as wheat straw (WS), which reaches almost five hundred million tons per year in China (Yang *et al.* 2013). The traditional disposal processes of composting and incineration cause air pollution and waste these abundant sources of lignocellulosic biomass.

WS is an ideal substitute raw material for woody biomass due to its similar structure (Yu *et al.* 2007) and properties; however, WS has a lower strength than woody biomass due to its low content of fibrous cells and high content of ash. Moreover, another challenge is the weak interfacial layer of the WS exterior surface owing to its large amount of waxes, silica, and lipophilic extractives (Jiang *et al.* 2009; Wen and Park 2013); therefore, it is difficult to achieve good mechanical strength with traditional adhesives (urea-formaldehyde resin and phenol-formaldehyde resin). Although methylene diphenyl diisocyanate (MDI) could be a good solution, it has higher costs and easily sticks to the platen press during manufacturing (Mo *et al.* 2003). For this technical

problem, various surface modifications of WS through different pretreatment methods have been studied, including mechanical (Pan *et al.* 2010), chemical (Kalia *et al.* 2009), thermal (Han *et al.* 2010; Li *et al.* 2011), and enzymatic methods (Jiang *et al.* 2009; Li *et al.* 2009) to improve its interface bonding performance. All these methods, however, decrease the intrinsic strength of WS, and effluent disposal results in additional pollution problems.

In recent years, controllable cold plasma as a new technology has been widely used in various material surface modifications (Busnel *et al.* 2010; Tang *et al.* 2012; Yang *et al.* 2014). Plasma is an ionized gas consisting of various charged particles. For WS, these energetic particles can destroy the weak interfacial layer *via* an etching process and introduce polar functional groups *via* an activated process. The effect of plasma treatment on the intrinsic strength of WS is negligible due to the short reaction depth. This fast, energy-saving, and pollution-free process has been used to modify material surfaces, with the most recent studies generally focusing on using $O_2$ as the feed gas in plasma treatment (Ma *et al.* 2010; Zhang *et al.* 2010). However, this is not conducive to industrial application, even though the surface modification has positive effects on the material.

In the current study, water vapor plasma was applied to the surface of WS to improve its adhesive permeability and mechanical properties. The changes in the WS from plasma treatment were characterized by measuring the surface wettability, shear strength, surface morphology, and surface chemical composition. Due to extensive sources of water vapor, this information is necessary for the development of the straw industry and waste utilization of high value-added products.

## EXPERIMENTAL

### Materials

Wheat straw (WS) was obtained from an agricultural field in the northern Jiangsu Province in China. After the WS was air-dried for several months, it was cleaned with distilled water to remove impurities from the surface and then cut into 5 cm-long pieces. Before plasma treatment, the WS samples were flattened and dried in a vacuum oven at 60 °C to a moisture content of 2%. All samples were kept in a desiccator to control the moisture content.

Urea-formaldehyde (UF) resin was used to evaluate the surface wettability and shear strength of the WS. It was prepared in a laboratory at Nanjing Forestry University. The major specifications of the UF resin were as follows: a solids content of 55% after drying at 120 °C for 2 h, a pH value of 7.0, and a viscosity of 28 mPa•s at 20 °C.

### Methods

*Water vapor plasma treatment*

Plasma treatments of the WS specimens were performed using a dielectric barrier discharge (DBD) produced from a plasma reactor (CTP-2000K, Suman Electronics Co., Ltd., Nanjing, China). The discharge power, chamber pressure, and treatment time are extremely important process parameters for water vapor plasma treatment. After a preliminary experiment, a discharge power of 40 W and a chamber pressure of 20 KPa were chosen because the filamentous current channel of the plasma under these conditions was stable and uniform. The primary focus of the experiments was to evaluate

the effect of treatment time on the WS surface. The flattened and dried WS specimens (5 mm × 50 mm) were placed inside of a vacuum chamber between two electrodes (Fig. 1). Before DBD discharge, the system was depressurized to 20 KPa, and a stable water vapor flow was maintained during gas flow. Treatment times of 60, 120, 180, and 240 s were tested.

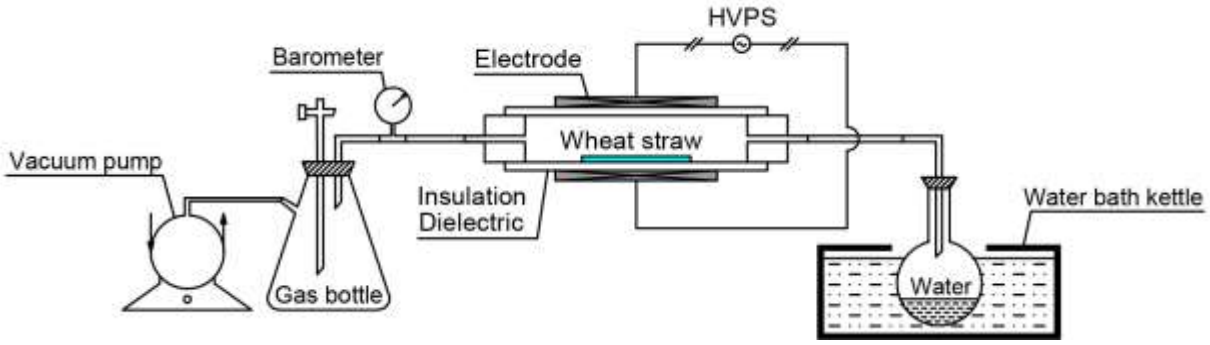


**Fig. 1.** Schematic representation of the water vapor plasma processor

*Contact angle measurement*

Liquid drop contact angle measurements were implemented using an optical contact angle measuring apparatus (Theta, Attension, Espoo, Finland). Drops of UF, distilled water, and diiodomethane (4 μL at 20 °C) were dispersed on the interior and exterior surfaces of the plasma-treated and untreated WS specimens. Ten replicates of the contact angle and surface free energy of wetting were measured for each type of specimen. Images of the drops on the specimens were captured using a camera connected to a computer. A photo was taken and saved every 50 ms. When the drop first landed on the surface, the images showed an instantaneous contact angle; as time elapsed, the drop flattened and stabilized, reaching an equilibrium contact angle.

*Shear strength evaluation*

A measurement model of shear strength was established previously (Yang *et al.* 2014). The shear strength was measured using a paper tension meter (WZL-300, Qingtong Boke Automation Technology Co., Ltd., Hangzhou, China) after the samples were cooled for at least 24 h. Two pieces of the untreated and plasma-treated WS specimens were coated with UF, then heated and pressed in a manual sheeter (32T, Zhenggong Co., Ltd., Dongguan, China). Twenty specimens were made for each sample type. The experimental conditions were as follows: specimen dimensions, 5 mm × 50 mm; gluing section, 5 mm × 15 mm; gluing type, interior-to-interior, interior-to-exterior, and exterior-to-exterior; resin content, 200 g/m$^2$; hot-pressing pressure, 1.5 MPa; hot-pressing temperature, 110 °C; and hot-pressing time, 90 s.

*Morphology observation by scanning electron microscopy (SEM)*

For SEM, the samples were cut into 5 mm × 5 mm squares. All WS specimens were placed in a vacuum drying oven at 60 °C and 0.1 Pa for 10 h. They were then transferred into the vacuum chamber for water vapor plasma treatment. After gold coating under vacuum, images of the WS interior and exterior surfaces were obtained with a JSM-7600F instrument (JEOL Ltd., Tokyo, Japan)

*Morphology observation by atomic force microscopy (AFM)*

AFM observations of the WS fibers were obtained using the Franklin maceration method. First, the WS samples were cut into 2 mm × 40 mm pieces and placed into boiling water until they sank to the bottom of the test tube. Next, the water was replaced with a solution of hydrogen peroxide and glacial acetic acid (volume ratio 1:1) and heated until the solution color turned white. Finally, the white floccus was washed with distilled water to a neutral condition and shaken to a fully dispersed form in a weighing bottle.

Before treatment with water vapor plasma, the distilled water drops containing the WS fibers were dripped onto clean mica sheets, placed in a spreading machine (KD-P, Kedi Instrumental Equipment Co., Ltd., Zhejiang, China) to eliminate the moisture, and moved to a vacuum drying oven at 40 °C for 2 h. After processing, the fiber-loaded mica sheets were attached to a stage for observation with an XE-100 instrument (Park Systems Inc., Suwon, Korea).

*Chemical composition analysis by X-ray photoelectron spectroscopy (XPS)*

The preparation of the WS specimens for XPS analysis was the same as for SEM. Information about the chemical structure of the treated and untreated WS surfaces was examined using a Shimadzu AXIS UltraDLD (Kyoto, Japan). The analysis room vacuum was 10E-9Pa, and the energy step size was 0.1 eV. A low-resolution spectrum was recorded from 0 to 1200 eV, and the C1 peaks from 270 to 300 eV were recorded at a high-resolution spectrum for deconvoluting into four components (C1, C2, C3, and C4).

## RESULTS AND DISCUSSION

### Effect of Water Vapor Plasma Treatment on Wettability of the WS Surface

The contact angle and the surface free energy indicate the wettability of solid materials (Aydin 2004). Therefore, the wettability of the WS interior and exterior surfaces before and after plasma treatment were analyzed in terms of these properties.

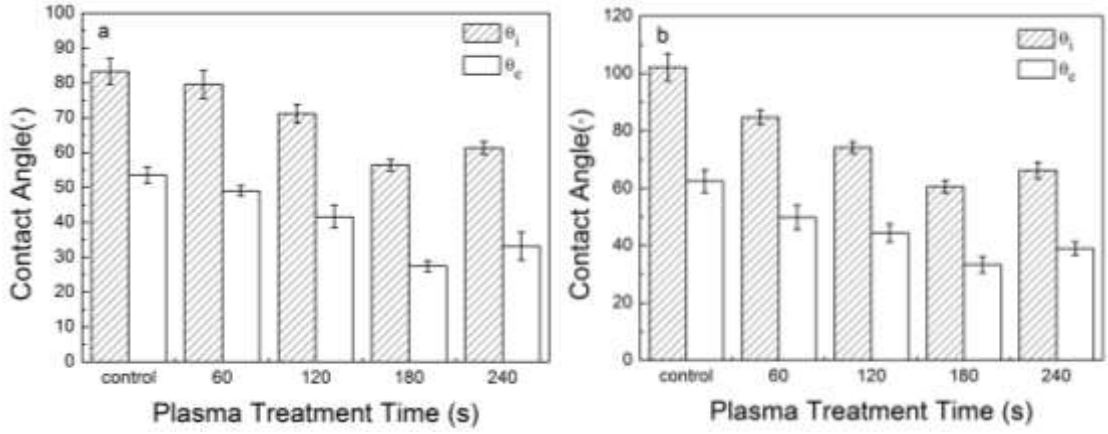


**Fig. 2.** The contact angles of the UF resin on the surfaces of the untreated and treated WS. (a) The interior surface and (b) the exterior surface, where $\theta$ represents the instantaneous contact angle and $\theta_e$ represents the equilibrium contact angle

*Contact angle of UF*

When a drop of UF resin was placed on the WS surface, an instantaneous contact angle was formed. The adhesive then spread over the straw surface and penetrated the WS body. Due to the high viscosity of the UF resin, this process was very slow, so 1000 s were allowed to reach the equilibrium contact angle. The instantaneous and equilibrium contact angles of the UF resin on both the interior and exterior surfaces of the plasma-treated and untreated specimens are shown in Fig. 2. The instantaneous and equilibrium contact angles on the exterior surface decreased by 17.1% and 20.3%, respectively, after water vapor plasma treatment for 60 s. The contact angles decreased with increasing treatment time from 60 s to 180 s. With 180 s of treatment, the contact angle decreased to a minimum that was much lower than those of the untreated specimens. For treatment times greater than 180 s, the instantaneous and equilibrium contact angles increased again. Thus, it was clear that the water vapor plasma treatment improved the wettability of the UF resin on the interior and exterior WS surfaces, and the best effect was obtained when the treatment time was 180 s.

In addition, a major difference existed in the contact angles between the interior and exterior WS surfaces. As shown in Fig. 2, the minimum equilibrium contact angles on the interior and exterior surfaces were 27.45° and 33.37°, respectively. The instantaneous contact angle of the interior and exterior surfaces decreased by 32.2% and 40.8% at best, respectively. This indicates that the wettability of the interior surface was greater than that of the exterior because of the different structures. The weak interfacial layer on the outer surface, which contained many cuticles, prevented the resin from spreading and penetrating into the surface (Liu *et al.* 2004; Ghaffar and Fan 2015).

The effect of plasma treatment for better wettability can be explained by an etching and active effect. The charged particles in the plasma system hit and degraded the aromatic or aliphatic polymers on the WS surface (Jamali and Evans 2011), which changed the microscopic morphology and increased the roughness of the WS surface; this process is known as etching. At the same time, many free radicals and active groups were generated, especially on the outer surface, partially from an electrochemical reaction and partially from the exposure inside the WS (Xu and Zhou 2009; Chen *et al.* 2010). Therefore, the interfacial polarity increased, and the wettability was enhanced. As the treatment time increased, the action time between the high-energy particles and the WS surface was longer, and thus the effect of etching and activation was more obvious, improving the wettability. However, when the concentration of free radicals and active groups on the WS surface became saturated after plasma treatment for 180 s, they could have been destroyed by the high-energy particles. The roughness of the nanoscale was therefore almost constant, and as a consequence, the wettability decreased again for a treatment time greater than 180 s. SEM, AFM, and XPS analyses were used to verify the accuracy of these conclusions.

**Table 1.** Surface Free Energy of the Untreated and Treated WS Specimens

| Treatment Time (s) | Surface Free Energy and its Components (mJ/m$^2$) | | | | | |
|---|---|---|---|---|---|---|
| | Exterior Surface | | | Interior Surface | | |
| | Total | Polarity | Dispersion | Total | Polarity | Dispersion |
| 0 | 34.96 | 7.55 | 27.41 | 40.20 | 11.89 | 28.31 |
| 60 | 46.45 | 19.5 | 26.95 | 55.05 | 31.34 | 23.91 |
| 120 | 51.24 | 22.97 | 28.27 | 59.17 | 27.82 | 31.35 |
| 180 | 58.12 | 31.25 | 26.87 | 66.20 | 39.47 | 26.73 |
| 240 | 52.16 | 26.34 | 25.82 | 57.11 | 32.86 | 24.25 |

*Surface free energy*

The surface free energy of the WS was calculated from the contact angle values of distilled water (polar liquid) and diiodomethane (non-polar liquid) using the Owens-Wendt method (Owens and Wendt 1969). The total free energy and its components of the inner and outer surface of the water vapor plasma treated and untreated specimens are shown in Table 1. For both the outer and inner surfaces, the total free energy increased initially and then decreased, which is in accordance with the polar component. After plasma treatment for 180 s, the largest increase rate of total free energy and the polar component of the outer surface were 66.2% and 313.9%, respectively. In addition, the dispersive component of the surface free energy slightly decreased. The rapid increase of the polar component is closely related to the generation of a large number of active groups. These changes corresponded to the contact angle analysis and verified the physical etching and chemical active effects.

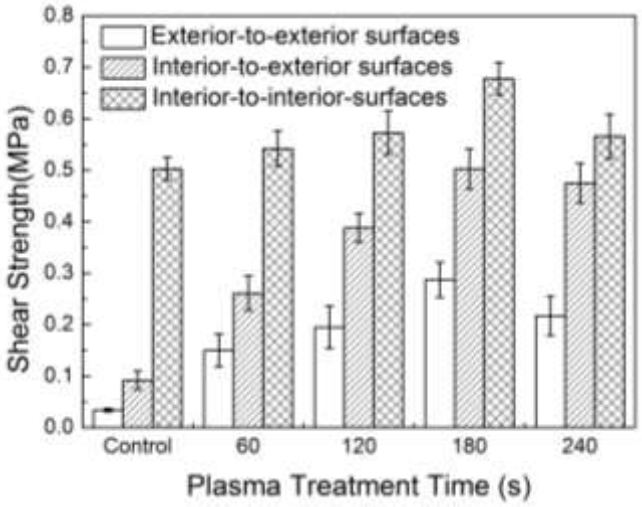


**Fig. 3.** Shear strength of the WS

## Effect of Water Vapor Plasma Treatment on the Interfacial Adhesion of WS with UF Resin

The shear strength measurements of the WS with UF resin are shown in Fig. 3. It is evident that the shear strength of the straw specimens with exterior-to-exterior surfaces, exterior-to-interior surfaces, and interior-to-interior surfaces dramatically improved after exposure to water vapor plasma treatment. Looking specifically at the treatment time of 180 s, the shear strength of the WS was 34.8%, 446.7%, and 744.1% greater than that of the untreated samples at the interior-to-interior, interior-to-exterior, and exterior-to-exterior surface, respectively. Particularly for the exterior-to-exterior

surface, which had a weak interface layer, there was nearly no shear strength (only 10% glued together) before plasma treatment. In addition, the shear strength increased initially and then decreased as the treatment time further increased. The specimens with 180 s of treatment had a higher shear strength than all other sample types. To correspond with wettability, the improvement in bonding of the WS surface confirmed the effect of water vapor plasma treatment.

## Effect of Water Vapor Plasma Treatment on the Morphology and Surface Roughness of WS

Surface roughness is a key factor that contributes to mechanical interlocking (Moghadamzadeh *et al*. 2011). In this study, two different methods were employed to display the WS topography before and after treatment with water vapor plasma: (i) SEM was used to observe the interior and exterior surfaces of the specimens and (ii) AFM was used to scan a 3 μm × 3 μm area of the WS fibers. Both methods clearly demonstrated the roughness of the WS surfaces.

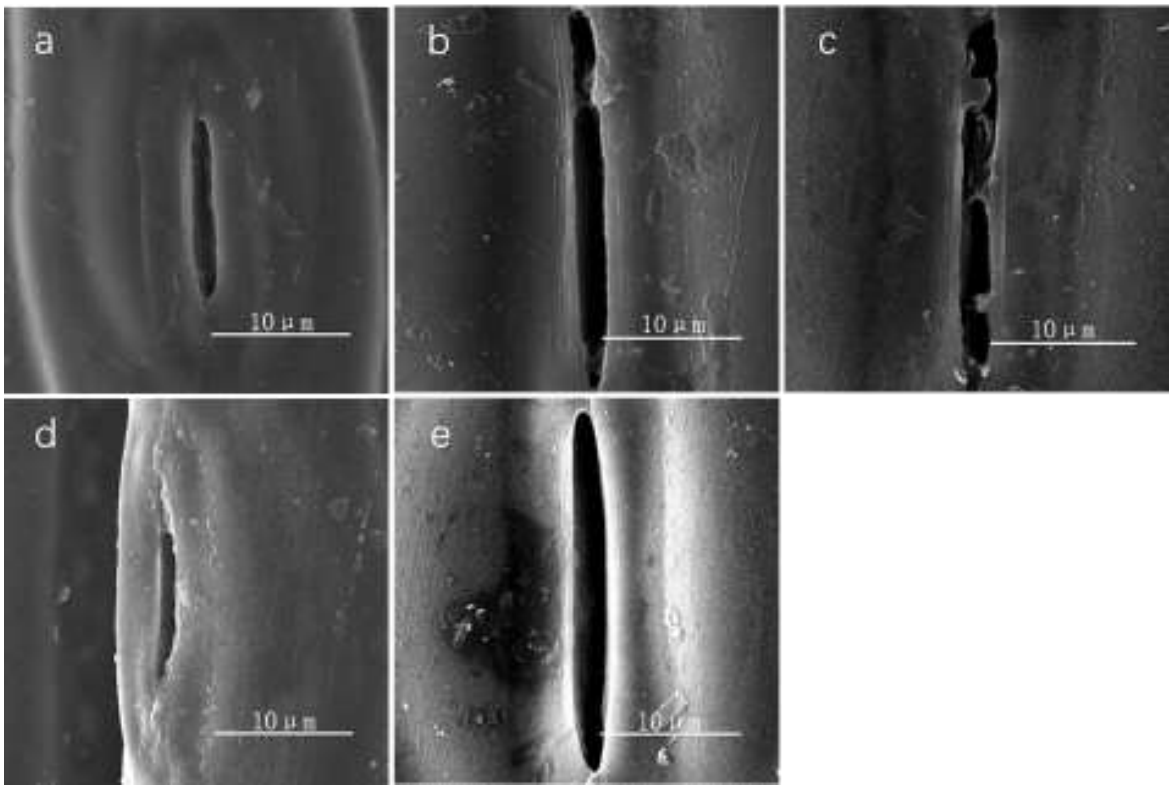


**Fig. 4.** Exterior surfaces of the WS observed under SEM: (a) untreated and water vapor plasma treatment of (b) 60 s, (c) 120 s, (d) 180 s, and (e) 240 s

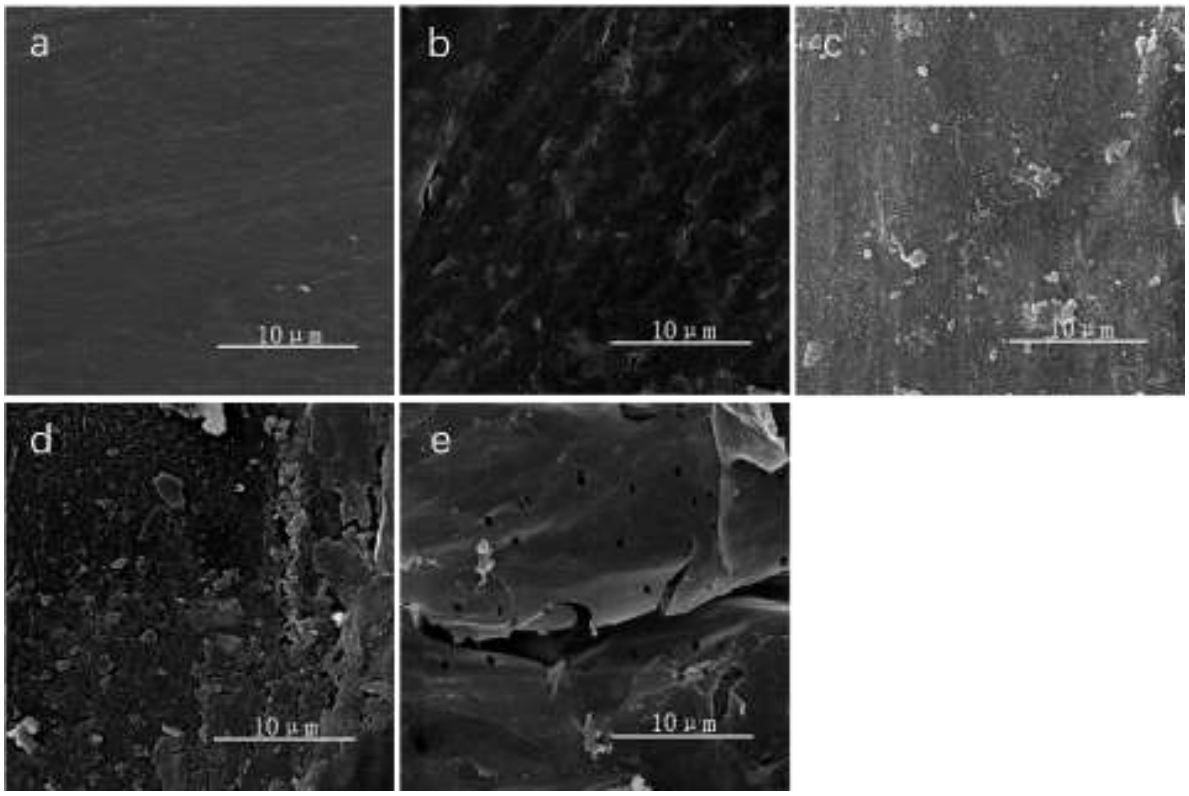


**Fig. 5.** Interior surfaces of the WS observed under SEM: (a) untreated and water vapor plasma treatment of (b) 60 s, (c) 120 s, (d) 180 s, and (e) 240 s

*SEM observation*

As illustrated in Figs. 4 and 5, for the untreated specimens, the SEM images showed that the interior and exterior surfaces were smooth and dense; however, the surfaces became rougher after water vapor plasma treatment. There were a lot of tiny nicks and grooves around the lenticels on the exterior surfaces. For the interior surfaces, a thin film structure that degenerated from the WS pith was shredded by the high-energy particle beam in the plasma system, and many dot notches appeared. The inner structure of the exposure and accessorial coarseness are favorable for UF resin anchoring. Additionally, as the treatment time increased, the nicks and grooves around the lenticels and notches on the interior surface became more obvious. Small holes appeared on the WS surfaces (Fig. 5), which was due to the long discharge time (over 180 s) being harmful to the bonding process. These phenomena were consistent with previous results.

*AFM observation*

Although the physical etching effect of the water vapor plasma treatment on the WS surfaces was observed by SEM, the images of the microstructure were only in two dimensions. AFM was therefore used to provide information of the microstructure in three dimensions. For observation analysis, AFM was used in combination with SEM to elucidate the influence of the water vapor plasma on the surface of the WS specimens.

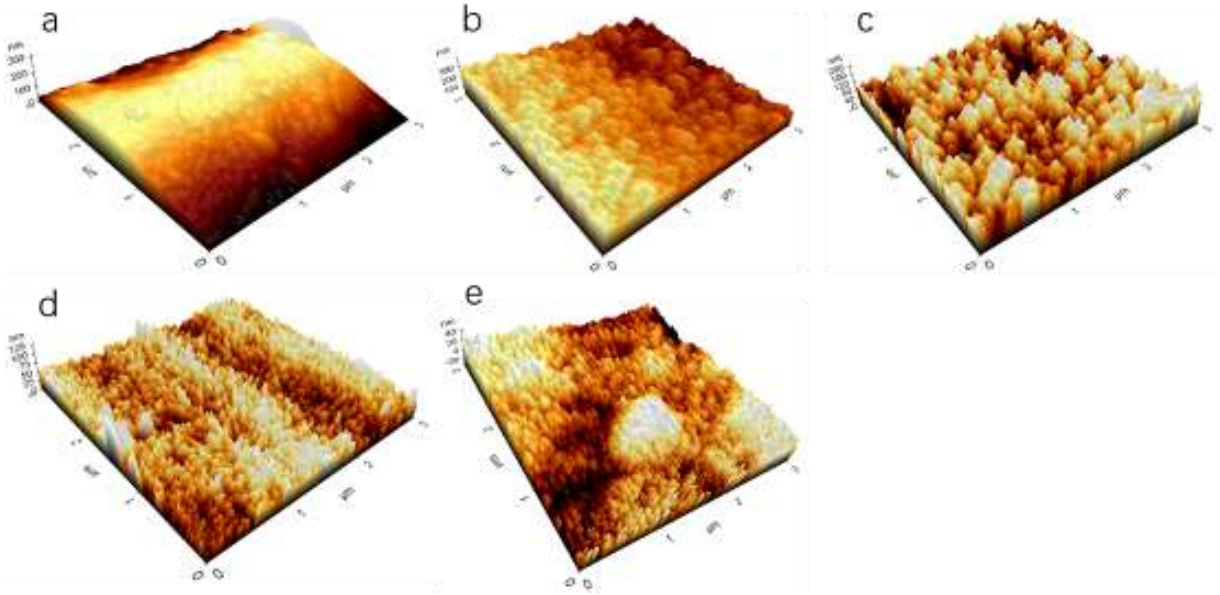


**Fig. 6.** 3D AFM images of the WS fibers. (a) untreated and water vapor plasma treatment of (b) 60 s, (c) 120 s, (d) 180 s, and (e) 240 s

Figure 6 shows the 3D images of the WS fibers before and after plasma treatment. A smooth arch can be seen on the fiber surface of the untreated specimens. In contrast, many uneven pits appeared on the fiber surfaces after water vapor plasma treatment. Moreover, as the treatment time increased, these indentations became more concentrated, and the concave and convex formations became sharper, especially for the treatment time of 180 s.

All these grooves on the nanoscale enhanced the bonding performance of the WS *via* the production of glue nails. However, when the treatment time was greater than 180 s, there was no nanoscale change in the roughness of the fiber surface; however, the thickness did decrease from 125 to 40 nm, which degrades the natural strength of WS. These conclusions were consistent with those of the shear strength analysis.

## Effect of Water Vapor Plasma Treatment on the Surface Chemistry of WS

As an effective characterization technique, XPS was applied to determine the qualitative and quantitative information for the chemical compositions and functional groups on the solid surfaces. For the WS specimens, a survey scan mode was performed to identify and quantify the basic elements (Fig. 7; Table 2). The carbon concentration gradually decreased with increasing treatment time, while the oxygen concentration increased correspondingly. The O/C ratio increased from 35.16% to 91.26% for the interior surface and from 8.08% to 66.72% for the exterior surface. Nevertheless, when the plasma treatment time was longer than 180 s, these measurements had an opposite trend. The most likely explanation for this is that the concentration of free radicals and active groups on the WS surface became saturated after plasma treatment for 180 s. Furthermore, the Si content initially increased and then decreased with a peak at 180 s.

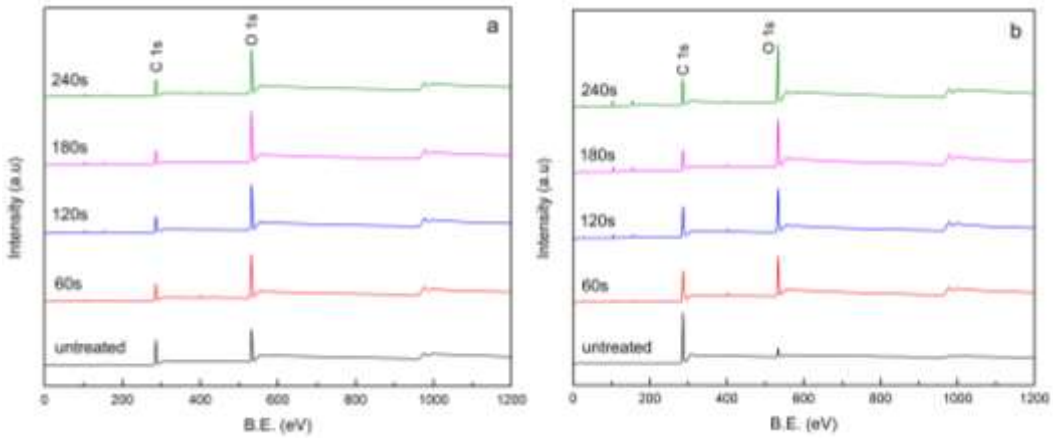


**Fig. 7.** XPS with survey scan mode for the WS before and after plasma treatment: (a) interior surface and (b) exterior surface

**Table 2.** Surface Atomic Concentration and O/C Ratios for the WS Specimens

| WS Samples | | Atomic Concentration (%) | | | |
|---|---|---|---|---|---|
| | | C | O | Si | O/C |
| Interior Surface | Untreated | 72.08 | 25.34 | 1.39 | 35.16 |
| | 60 s | 57.69 | 36.77 | 1.48 | 63.74 |
| | 120 s | 54.47 | 39.71 | 4.65 | 72.90 |
| | 180 s | 47.01 | 42.90 | 7.77 | 91.26 |
| | 240 s | 56.30 | 36.76 | 4.27 | 65.29 |
| Exterior Surface | Untreated | 90.99 | 7.35 | 0.73 | 8.08 |
| | 60 s | 68.61 | 25.34 | 2.45 | 36.93 |
| | 120 s | 66.04 | 26.54 | 4.40 | 40.19 |
| | 180 s | 53.09 | 35.42 | 8.25 | 66.72 |
| | 240 s | 57.59 | 33.07 | 7.65 | 57.42 |

XPS with deconvolution analysis of the C1 peaks was performed to identify and quantify the chemical functional groups introduced by the plasma reaction. The results of the analysis are shown in Fig. 8 and Table 3. The C1, C2, C3, and C4 peaks were assigned to C=C/C-C/CHx, -C-OR, C=O, and –COO groups, respectively. The results showed that the WS with a 180 s treatment time had lower C1 content and higher C3 and C4 contents than the specimens of other treatment times. This data indicates that the introduction of massive oxygen-containing functional groups occurred during the water vapor plasma treatment and that 180 s of treatment was sufficient to increase the wettability and permeation of the UF resin. These conclusions are in agreement with the changes of the surface free energy and contact angles.

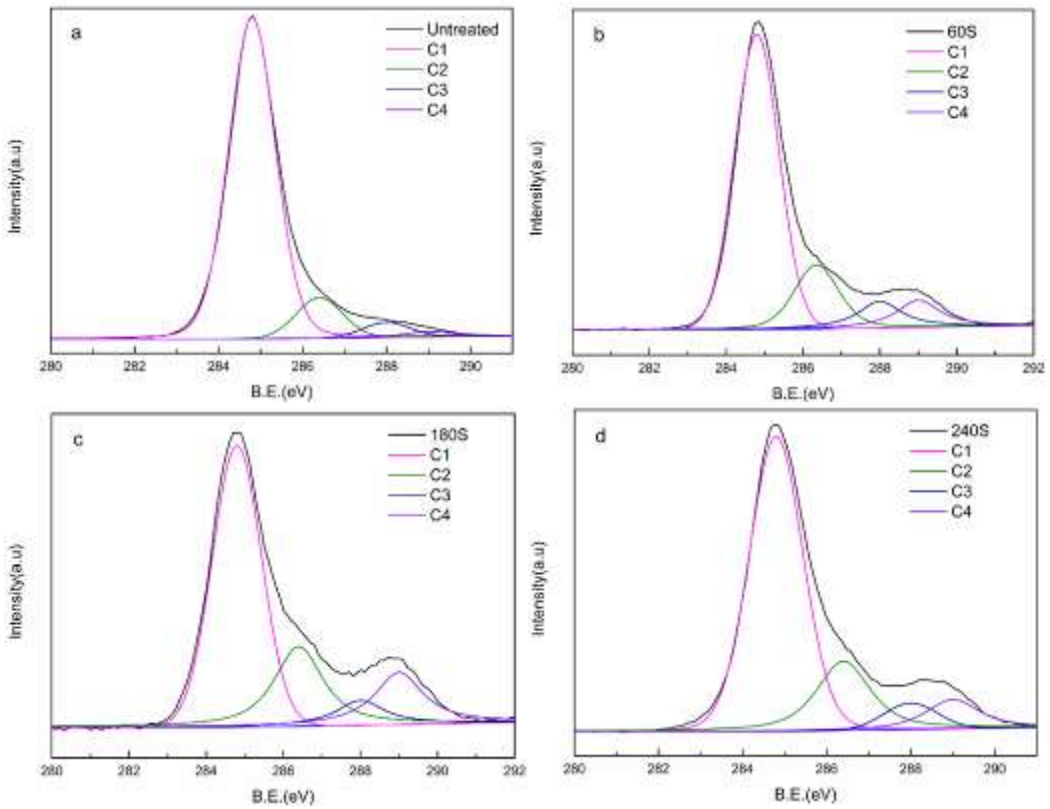


**Fig. 8.** C1 curve fitting for the exterior surface of the WS: (a) untreated and water vapor plasma treatment of (b) 60 s, (c) 180 s, and (d) 240 s

**Table 3.** Test Data for the C1 Peak of the WS Specimens

| WS Samples | | C1s Components (%) | | | |
|---|---|---|---|---|---|
| | | C1 | C2 | C3 | C4 |
| Interior Surface | Untreated | 40.72 | 48.36 | 9.96 | 0.96 |
| | 60 s | 38.63 | 43.69 | 14.45 | 3.23 |
| | 120 s | 25.62 | 49.71 | 16.87 | 7.80 |
| | 180 s | 26.69 | 35.14 | 22.38 | 15.79 |
| | 240 s | 29.55 | 47.82 | 16.31 | 6.32 |
| Exterior Surface | Untreated | 84.52 | 10.22 | 3.67 | 1.59 |
| | 60 s | 66.06 | 16.51 | 8.70 | 8.73 |
| | 120 s | 67.05 | 18.05 | 6.00 | 8.90 |
| | 180 s | 55.61 | 21.89 | 7.25 | 15.25 |
| | 240 s | 66.07 | 19.76 | 5.69 | 8.48 |

From the above discussion, the effect of water vapor plasma modification on the WS surface could be divided into two simultaneous aspects: physical etching and electrochemical activation. Although the treatment time was prolonged from 0 to 240 s, the process took place step-by-step (Fig. 9). Step 1 represents the treatment until 60 s. The weak interfacial layer (b) on the exterior surface of the WS was the first to be bombarded with high-energy particles in the plasma system, which caused long

hydrocarbon chain scission and some tiny silicon and wax crystals to be cut from the epidermal cell. At the same time, a large number of oxygen free radicals and ions (such as •OH, ⁻OH, and $OH^-$) in the water vapor plasma became enriched and reacted with the fragmented chain through new chemical bonds, which increased the surface polarity. However, after 60 s, the weak interfacial layer was not completely etched away. Step 2 occurred during the treatment time of 60 to 120 s, for which etching reached the inner layer and the chemical activation was more complete. In Step 3, which represents 120 to 180 s, the weak interface layer was completely chipped off. The surface structure became finer, while the electrochemical reaction achieved saturation. In Step 4, with further etching from 180 s to 240 s, the roughness remained nearly constant, but the thickness of the inner layer decreased, which negatively impacted the intrinsic strength of the WS. Additionally, the surface polarity decreased again due to the destruction of oxygen-containing functional groups by long-irradiation. All these steps were reflected in the bonding strength after gluing.

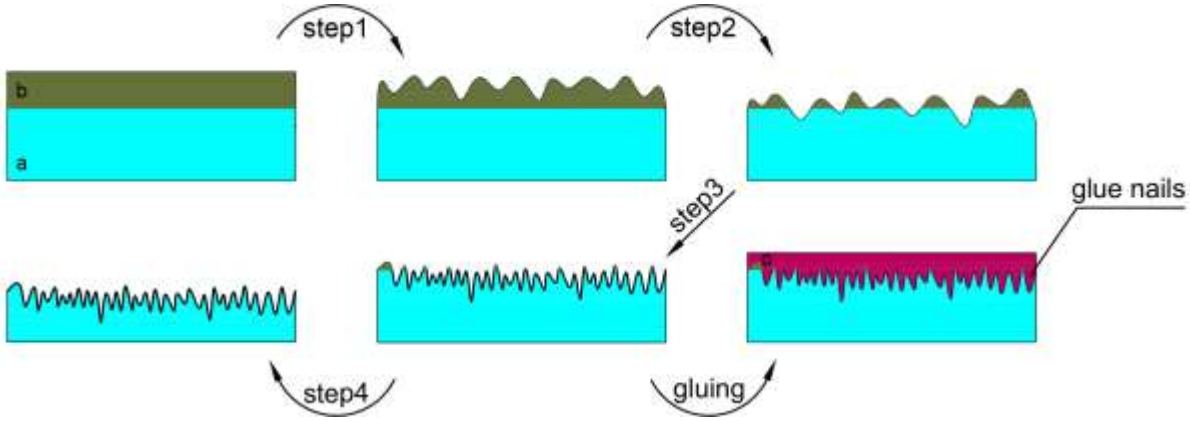


**Fig. 9.** Schematic diagram of the plasma reaction process: (a) endothecium of WS and (b) weak interface layer

## CONCLUSIONS

1. The interior surface of the WS had a higher wettability than the exterior surface, with or without water vapor plasma treatment.
2. The water vapor plasma treatment provided an effective method of improving the surface properties of the WS, which allowed for the UF resin to penetrate into the WS body and produce strong adhesion.
3. As the treatment time increased, the wettability and shear strength of the WS surfaces increased at first and then decreased. The optimal treatment time for water vapor plasma was 180 s.
4. The changes in the microscopic topography and chemical composition of the WS surfaces are powerful evidence for the better wettability.

## ACKNOWLEDGMENTS

The authors are grateful for the support of projects from the National Natural Science Foundation of China (Grant No. 31270606) and Priority Academic Program Development of Jiangsu Higher Education Institutions (PAPD). This work was also sponsored by the Qing Lan Project. Sincere thanks go to Jiangsu Engineering Research Center of Fast-growing Trees and Agri-fiber Materials for providing equipment for this study.

## REFERENCES CITED

Aydin, I. (2004). "Activation of wood surfaces for glue bonds by mechanical pre-treatment and its effects on some properties of veneer surfaces and plywood panels," *J. Appl. Surf. Sci.* 233(1-4), 268-274. DOI: 10.1016/j.apsusc.2004.03.230

Busnel, F., Blanchard, V., Prégent, J., Stafford, L., Riedl, B., Blanchet, P., Sarkissian, A., and Riedl, P. B. A. S. (2010). "Modification of sugar maple (*Acer saccharum*) and black spruce (*Picea mariana*) wood surfaces in a dielectric barrier discharge (DBD) at atmospheric pressure," *J. Adhes. Sci. Technol.* 24(8-10), 1401-1413. DOI: 10.1163/016942410X501007

Chen, G., Xiang, S., and Zhou, L. (2010). "Surface modification of corn stalk by low temperature plasma," *Journal of Central South University of Forestry & Technology* 30(8), 92-95. DOI: 10.14067/j.cnki.1673-923x.2010.08.001

Damette, O., and Delacote, P. (2011). "Unsustainable timber harvesting, deforestation and the role of certification," *Ecol. Econ.* 70(6), 1211-1219. DOI: 10.1016/j.ecolecon.2011.01.025

Ghaffar, S. H., and Fan, M. (2015). "Differential behaviour of nodes and internodes of wheat straw with various pre-treatments," *Biomass Bioenerg.* 83, 373-382. DOI: 10.1016/j.biombioe.2015.10.020

Han, G., Deng, J., Zhang, S., Bicho, P., and Wu, Q. (2010). "Effect of steam explosion treatment on characteristics of wheat straw," *Ind. Crop Prod.* 31(1), 28-33. DOI: 10.1016/j.indcrop.2009.08.003

Jamali, A., and Evans, P. D. (2011). "Etching of wood surfaces by glow discharge plasma," *Wood. Sci. Technol.* 45(1), 169-182. DOI: 10.1007/s00226-010-0317-7

Jiang, H., Zhang, Y., and Wang, X. (2009). "Effect of lipases on the surface properties of wheat straw," *Ind. Crop Prod.* 30(2), 304-310. DOI: 10.1016/j.indcrop.2009.05.009

Kalia, S., Kaith, B. S., and Kaur, I. (2009). "Pretreatments of natural fibers and their application as reinforcing material in polymer composites - A review," *Polym. Eng. Sci.* 49(7), 1253-1272. DOI: 10.1002/pen.21328

Li, X., Cai, Z., Winandy, J. E., and Basta, A. H. (2011). "Effect of oxalic acid and steam pretreatment on the primary properties of UF-bonded rice straw particleboards," *Ind. Crop Prod.* 33(3), 665-669. DOI: 10.1016/j.indcrop.2011.01.004

Li, Y., Pickering, K. L., and Farrell, R. L. (2009). "Analysis of green hemp fibre reinforced composites using bag retting and white rot fungal treatments," *Ind. Crop Prod.* 29(2-3), 420-426. DOI: 10.1016/j.indcrop.2008.08.005

Liu, Z., Wang, F., and Wang, X. (2004). "Surface structure and dynamic adhesive wettability of wheat straw," *Wood & Fiber Sci.* 36(2), 239-249.

Ma, K., Chen, P., Wang, B., Cui, G., and Xu, X. (2010). "A study of the effect of oxygen plasma treatment on the interfacial properties of carbon fiber/epoxy composites," *J. Appl. Polym. Sci.* 118(3), 1606-1614. DOI: 10.1002/app.32549

Moghadamzadeh, H., Rahimi, H., Asadollahzadeh, M., and Hemmati, A. R. (2011). "Surface treatment of wood polymer composites for adhesive bonding," *International Journal of Adhesion & Adhesives* 31(8), 816-821. DOI: 10.1016/j.ijadhadh.2011.08.001

Mo, X., Cheng, E., Wang, D., and Sun, X. S. (2003). "Physical properties of medium-density wheat straw particleboard using different adhesives," *Ind. Crop Prod.* 18(1), 47-53. DOI: 10.1016/S0926-6690(03)00032-3

Owens, D. K., and Wendt, R. C. (1969). "Estimation of the surface free energy of polymers," *J. Appl. Polym. Sci.* 13, 1741-1747. DOI: 10.1002/app.1969.070130815

Pan, M., Zhou, D., Zhou, X., and Lian, Z. (2010). "Improvement of straw surface characteristics via thermomechanical and chemical treatments," *Bioresource Technol.* 101(20), 7930-7934. DOI: 10.1016/j.biortech.2010.05.022

Tang, L., Zhang, R., Zhou, X., Pan, M., Chen, M., Yang, X., Zhou, P., and Chen, Z. (2012). "Dynamic adhesive wettability of poplar veneer with cold oxygen plasma treatment," *BioResources* 7(3), 3327-3339. DOI: 10.15376/biores.7.3.3327-3339

Wen, M., Shi, J., and Park, H. (2013). "Dynamic wettability and curing characteristics of liquefied bark-modified phenol formaldehyde resin (BPF) on rice straw surfaces," *J. Wood Sci.* 59(3), 262-268. DOI: 10.1007/s10086-013-1329-3

Xu, X., and Zhou, D. (2009). "XPS analysis of rice straw modified with plasma treatment," *Journal of Nanjing Forestry University (Natural Science Edition)* 33(5), 69-72.

Xu, X., Zhou, D., Wu, Q., and Vlosky, R. P. (2004). "Agri-based composites in China: Opportunities and challenges," *Forest Prod. J.* 54(5), 8-15.

Yang, X., Tang, L., Zhang, R., and Zhou, X. (2013). "Review on progress of crop straws surface modification," *Journal of Nanjing Forestry University (Natural Sciences Edition)* 37(3), 157-162.

Yang, X., Zhang, R., Tang, L., Chen, M., Li, Y., and Zhou, X. (2014). "Dynamic wettability of different adhesives on wheat straw surface modified by cold oxygen plasma treatment," *BioResources* 9(1), 1578-1587. DOI: 10.15376/biores.9.1.1578-1587

Yildirim, H. T., Candan, Z., and Korkut, S. (2014). "Wood-based panels industry in Turkey: Future raw material challenges and suggestions," *Maderas: Ciencia y Tecnología* 16(2), 175-186. DOI: 10.4067/S0718-221X2014005000014

Yu, H., Liu, R., Qiu, L., and Huang, Y. (2007). "Composition of the cell wall in the stem and leaf sheath of wheat straw," *J. Appl. Polym. Sci.* 104(2), 1236-1240. DOI: 10.1002/app.25755

Zhang, R., Tang, L., Qian, Y., Xu, J., and Zhou, X. (2010). "The effect of oxygen cold plasma treatement on surface wettability of poplar veneers," *Wood Processing Machinery* 21(4), 25-27. DOI: 10.13594/j.cnki.mcjgjx.2010.04.004

Article submitted: April 17, 2016; Peer review completed: June 12, 2016; Revised version received and accepted: October 17, 2016; Published: January 10, 2017.
DOI: 10.15376/biores.12.1.1403-1416